



## Structural and spectroscopic characterization of HgS nanoparticles prepared via simple microwave approach in presence of novel sulfuring agent

Hossein SAFARDOUST-HOJAGHAN<sup>1</sup>, Maryam SHAKOURI-ARANI<sup>2</sup>, Masoud SALAVATI-NIASARI<sup>1</sup>

1. Institute of Nano Science and Nano Technology, University of Kashan, Kashan, P.O. Box 87317-51167, Iran;

2. Department of Chemistry, Payame Noor University, Tehran, P.O. Box 19395-3697, Iran

Received 23 April 2015; accepted 4 August 2015

**Abstract:** Mercury sulfide (HgS) crystals with different morphologies and particle sizes, were obtained via a simple microwave reaction by a new precursor complex, [bis ((2-suphanylphenyl)imino)methylphenol] Hg(II) ( $[\text{Hg}(\text{C}_{13}\text{H}_{11}\text{NSO})_2]^{2+}$ ). The products were characterized by X-ray diffraction (XRD), scanning electron microscopy (SEM), ultraviolet–visible (UV–Vis) spectroscopy. Mercury sulfide nanostructures with different sizes were prepared. The effects of precursor concentration, type of solvent, microwave time, and power on the particle size and morphology were investigated. The results show that the type of solvent and microwave power play key roles in the final size of HgS. Ethylene glycol is the best solvent for the synthesis of very fine particles of HgS, and the best power for the preparation of HgS nanoparticles with uniform size distribution is 900 W. The band gap for HgS nanoparticles calculated by UV–Vis spectrum was 3.2 eV which had about 1.2 eV blue shift in comparison with the band gap of 2 eV for bulk sample.

**Key words:** mercury sulfide; microwave method; nanostructures; thio Schiff-base

### 1 Introduction

Intensive researches have been conducted on nanocrystalline chalcogenides due to their unique thermoelectric, optical and semiconducting properties. Chalcogenide compounds belonging to the II–VI family have been extensively studied for their nonlinear optical optoelectronic and photochemical applications, and represent ideal systems for dimension-dependent properties [1–5]. On the other hand, only a few studies have reported the preparation of HgS, due to the high toxicity problem of mercury. Nevertheless, mercury sulfide is a promising material with wide application in many fields including image sensors, electrostatic image materials, infrared detectors, catalysts [6] and light emitting diodes [7,8]. The application of mercury sulfide in catalysts and infrared detector is due to its narrow gap band [9]. The crystalline forms of mercury sulfide are the cubic phase ( $\beta$ -HgS, metacinnabar) and the hexagonal phase ( $\alpha$ -HgS, cinnabar). So far, HgS nanostructures have been reported with various morphologies and architectures, such as tube-like particles [10], star-shape [11], rod-like particles [12], nanoparticles [13–16]

and dendrites [17].

Various techniques have been developed for the synthesis of semiconductor, e.g., micro and nano size HgS, mainly including micelle and microemulsion templates [13], microwave irradiation [10], sol–gel template [18], hydrothermal method [17], solid state reaction at high temperatures [19,20], Langmuir–Blodgett (LB) method [21,22], gas reaction and so on. Among different routes, microwave method is the best method because it is a green method and consumes less energy and time.

The microwave method is another novel method to fabricate lead and mercury sulfides, and lead sulfate [23,24] is a very rapidly developing area of research. It is well known that microwaves are electromagnetic waves containing electric and magnetic field components. The charged particles start to migrate or rotate when the electric field applies a force on the charged particles. Further polarization of polar particles takes place because of the movement of charged particles. The concerted forces applied by the electric and magnetic components of microwave change in direction, which creates the attrition and collisions of molecules. Thermal and non-thermal effects are claimed effects of

microwave irradiation [25].

In recent years, microwave irradiation have been extensively used to fabricate novel materials with unusual properties. This method, as a heating route, is generally quite fast, simple and efficient in energy, can induce the formation of particles with a much smaller size and higher surface area [26].

LI et al [27] have prepared mercury chalcogenides HgE (E=S, Se, Te) with spherical morphologies in ethylenediamine at room temperature [27]. YANG et al [28] have prepared metal sulfide using thioglycolic acids (TGA) as nontoxic template with a mild hydrothermal route.

In this study, one novel route based on microwave-included method for the synthesis of nanocrystalline HgS using a new sulfuring agent from classes of thio Schiff-base in different solvents was studied and the product was characterized by powder X-ray diffraction (XRD), scanning electron microscopy (SEM), transmission electron microscopy (TEM) and energy dispersive X-ray analysis (EDX).

## 2 Experimental

### 2.1 Materials and physical measurements

All chemicals were of analytical grade and used as-received without further purification. XRD patterns were recorded by a Rigaku D-max C III X-ray diffractometer using Ni-filtered Cu  $K_{\alpha}$  radiation. Gas chromatography (GC-2550TG, Teif Gostar Faraz Company, Iran) was used for all chemical analyses. The compositional analysis was done by energy dispersive X-ray analysis (EDX, KeveX, Delta Class I). Scanning electron microscopy (SEM) images were obtained on a Philips XL-30E SEM equipped with energy dispersive X-ray spectroscopy. Fourier transform infrared (FT-IR) spectra were recorded on a Shimadzu Varian 4300 spectrophotometer in KBr pellets. The electronic spectra of the complexes were taken on a Shimadzu UV-visible scanning spectrometer (Model 2101 PC).

### 2.2 Preparation of HgS nanoparticles

In a typical procedure, HgS nanoparticles were prepared as follows: during the first step, proper amount of salicylaldehydes were added to 2-aminothiophenol solution (molar ratio of salicylaldehyde to 2-aminothiophenol is 1:1) and the mixture was stirred for 30 min. At the end of this step, the precipitate was centrifuged and washed with methanol and finally dried in a vacuum oven at 40 °C for 5 h. During a second step, 0.431 g prepared ligand in earlier stages was dissolved in propyleneglycol (20 mL) under stirring, and was added to 0.3 g mercury(II) acetate solution and then stirred for 60 min. Afterwards, the final solution was left for cyclic

microwave radiation at different powers in different solvents for different exposure time. Each cycle was 90 s long and composed of 30 and 60 s for the on and off periods, respectively. At the end of reaction, the HgS nanoparticles suspension was cooled to room temperature, the solvent was removed by centrifugation and the HgS nanoparticles were washed several times with ethanol, dried in a vacuum oven at 50 °C for 5 h. Table 1 shows the experimental conditions for the preparation of HgS nanoparticles.

**Table 1** Products obtained under different conditions

Sample	Microwave power/W	Molar ratio of Hg <sup>2+</sup> to thio Schiff-base	Time/min	Solvent
1	600	0.5	5	PG
2	750	0.5	5	PG
3	900	0.5	5	PG
4	900	0.25	5	PG
5	900	0.5	10	PG
6	900	0.5	15	PG
7	900	0.5	5	H <sub>2</sub> O
8	900	0.5	5	EG

## 3 Results and discussion

HgS nanoparticles can be prepared by the addition of thio Schiff-base (described above) into Hg(OAc)<sub>2</sub> solution at ambient temperature and by conventional heating and microwave heating methods resulted in the formation of HgS nanoparticles (space group:  $F\bar{4}3m$ ). Figure 1 shows the typical XRD pattern of sample synthesized with microwave oven power of 900 W for 5 min. The particles are crystalline with no peaks attributable to Hg(OAc)<sub>2</sub>, and thio Schiff-base and HgO are observed. All of the peaks in the XRD pattern can be indexed as cubic phase with calculated lattice parameters

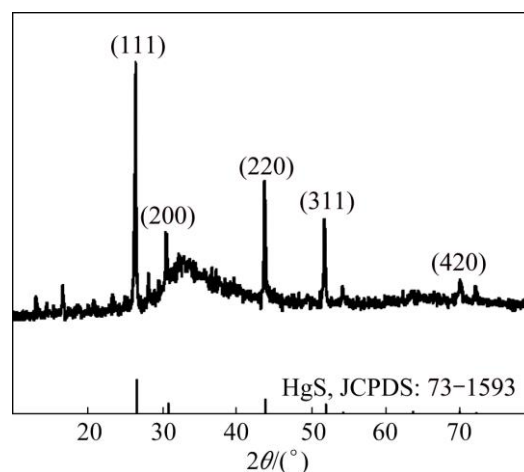


**Fig. 1** XRD pattern of HgS obtained at 900 W for 5 min

of  $a=b=c=5.8717 \text{ \AA}$ , which agree well with the reported values for HgS (JCPDS Card No. 73–1593). The average size of HgS nanoparticles synthesized by conventional heating method is calculated to be approximately 38.5 nm, according to Debye Scherrer formula [29]:  $D=0.9\lambda/\beta\cos\theta$ , where  $\beta$  is the FWHM (full-width at half-maximum) in radian;  $\theta$  is the Bragg angle and  $\lambda$  is the X-ray wavelength (1.5406  $\text{\AA}$  for Cu  $K_{\alpha}$ ) [30].

Hg(OAc)<sub>2</sub> and thio Schiff-base (C<sub>13</sub>H<sub>11</sub>NSO) were mixed in propylene glycol (PG) and stirred at ambient temperature. The formation mechanism for this synthesis is schematically presented in Scheme 1. It can be seen that as the reaction processes, [(2-suphanylphenyl imino) methylphenol] forms a complex with Hg via its OH and SH groups. Then, this complex is ruptured under microwave irradiation and HgS is produced.

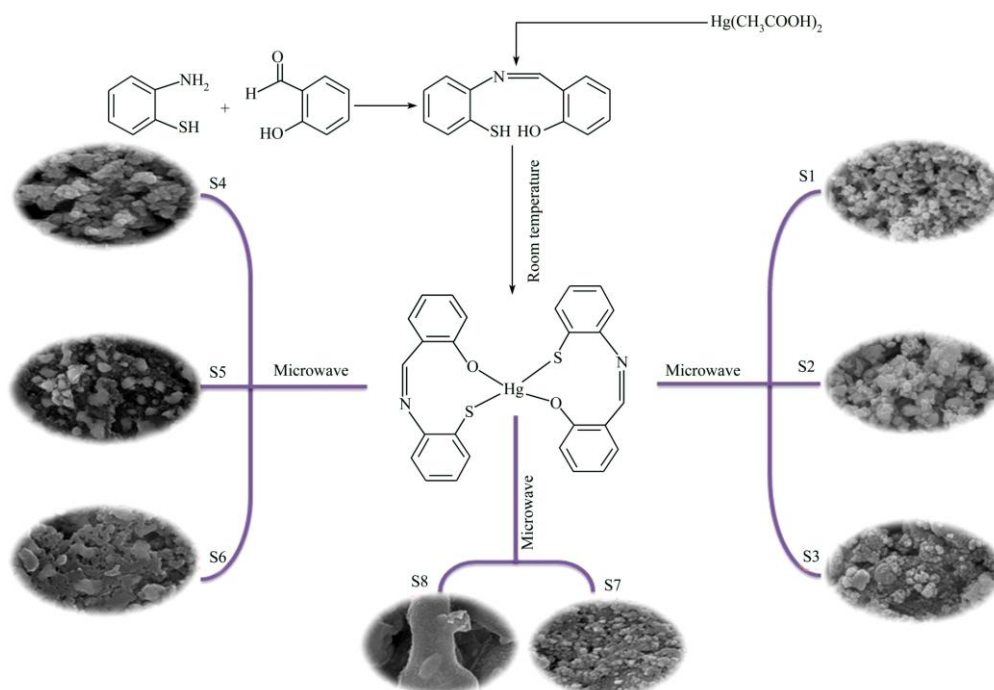
To study whether the surface of as-synthesized HgS was capped with organic surface, FT-IR detection of as-synthesized samples was performed. The FT-IR spectra of as-synthesized thio Schiff-base, the complexed species of Hg(C<sub>13</sub>H<sub>11</sub>NSO)<sub>2</sub><sup>2+</sup> and synthesized products with microwave oven power of 900 W for 5 min with microwave processing are shown in Fig. 2.

For the produced thio Schiff-base (Fig. 2(a)), the band at 2600  $\text{cm}^{-1}$  corresponds to the S—H stretch vibration, and the bands at 1614 and 752  $\text{cm}^{-1}$  are related to the C=N and C—S stretching, respectively. The peaks from 1583 to 1489  $\text{cm}^{-1}$  are C=C aromatic stretching vibrations and the band at 3255  $\text{cm}^{-1}$  corresponds to the N—H stretch vibration. Figure 2(b) is related to the complex prepared from mercury(II) acetate and respective ligand which shows that the number and

intensities of peaks are diminished because the product symmetry increases. Therefore, it can be concluded that the complex forms and the stretch vibrations at 1612, 1384, 750, 557, 466  $\text{cm}^{-1}$  attribute to the C=N, C=C, C—S, Hg—N and Hg—S stretching models of complex, respectively. However, the FT-IR spectrum of as-synthesized HgS (Fig. 2(c)) does not show any obvious evidence in the S—H vibration mode range, which proves that the thio Schiff-base are bonded to the Hg(OAc)<sub>2</sub> through sulfide group, and the disappearance of S—H and C=C, N—H, C—N and C—S peaks in Fig. 2(c) can prove the explanation above. Figure 2(c) has no absorption peaks in the range of 4000–500  $\text{cm}^{-1}$ , so pure HgS product was synthesized without any impurities. Therefore, these peaks (positioned at 3445 and 1615  $\text{cm}^{-1}$ ) must be caused by O—H stretching models and insignificant amount of thio Schiff-base molecule was absorbed on the surface of HgS.

A typical EDX spectrum of sample prepared at microwave oven power of 900 W for 5 min in propylene glycol is shown in Fig. 3, which indicates the presence of Hg and S in the product. According to the calculation of peak areas, the molar ratio of Hg to S is 57.71:42.29, which is very close to the stoichiometric ratio of HgS. Therefore, both XRD and EDX analyses show that pure HgS nanoparticles are produced via the present synthetic method.

Figure 4 shows the SEM images of products produced by a microwave approach for different exposure time. The microwave time also plays an important role in the morphology of product. When the reaction time was maintained at 5 min and other



**Scheme 1** Reaction condition for preparing products

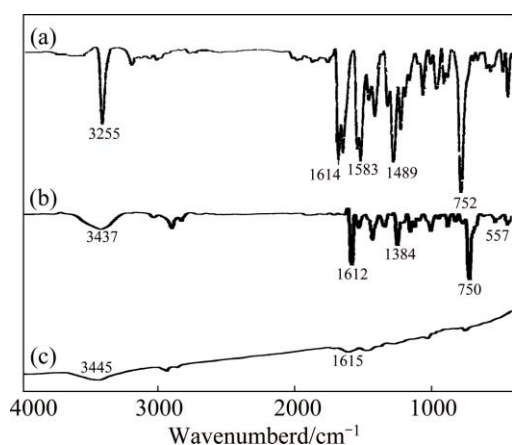


**Fig. 2** FT-IR spectra of as-synthesized thio Schiff-base ligand (a), complex from lead(II) nitrate and ligand (b), and HgS sample (c) at 900 W for 5 min

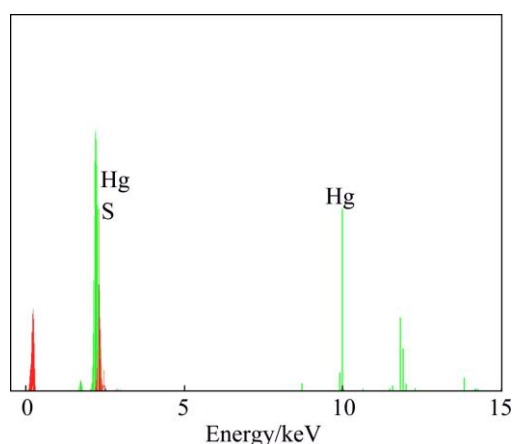


**Fig. 3** EDX spectrum of HgS synthesized at 900 W for 5 min

conditions were constant (microwave oven power of 900 W, propylene glycol as solvent), HgS nanoparticles with very tiny particles was obtained, indicating that 5 min is the proper time for the synthesis of nanoparticles (Fig. 4(a)). By increasing the reaction time, bulk of irregular masses as well as some nanoparticles form (Fig. 4(b)). So, it can be concluded that this duration is not favored for the formation of nanoparticles. At 15 min, large and impacted particles with 100–150 nm in diameters are obtained, which reveals that for this duration, due to higher amount of energy provided by microwave, more nucleation occurs and larger particles are obtained (Fig. 4(c)).

The microwave power directly affects the temperature of reaction solution, and higher applied power results in higher temperature [31]. Figure 5 illustrates the influence of microwave power on the morphology and particle size. It is found that the best power for the preparation of HgS nanoparticles with uniform size distribution is 900W (Fig. 5(c)). At lower power (600 and 750 W), due to low energy and

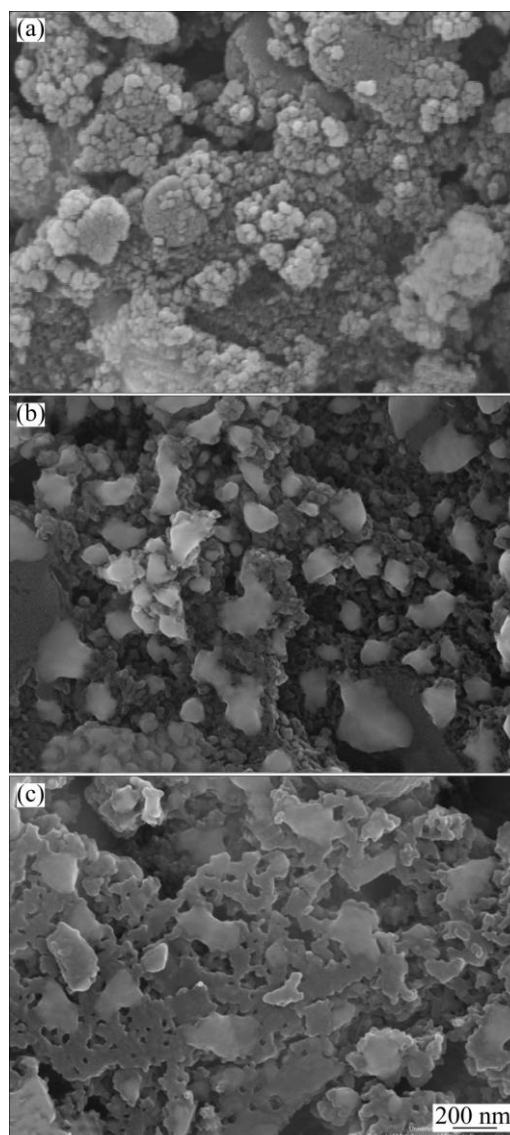


**Fig. 4** SEM images of products synthesized at 900 W for 5 min (a), 10 min (b) and 15 min (c)

temperature, agglomerated and bulky masses have been achieved (Figs. 5(a) and (b)). Also some ball-like structures can be seen in these samples. By increasing the power, the temperature of microwave increases. In fact, at power of 900 W, microwave can provide required energy for the formation of product with small and proper size and morphology.

The solvents due to different physical and chemical properties can influence the solubility, reactivity, and diffusion behaviors of reactants. In particular, the polarity and coordinating ability of solvent can influence the crystal shape of final product [32–34]. Solvents, due to different polarities and boiling points [35], can affect the rates of nucleation, growth, morphology and size of final product. Microwave chemistry is based on the effective heating of material by microwave dielectric heating that depend on the ability of material (solvent

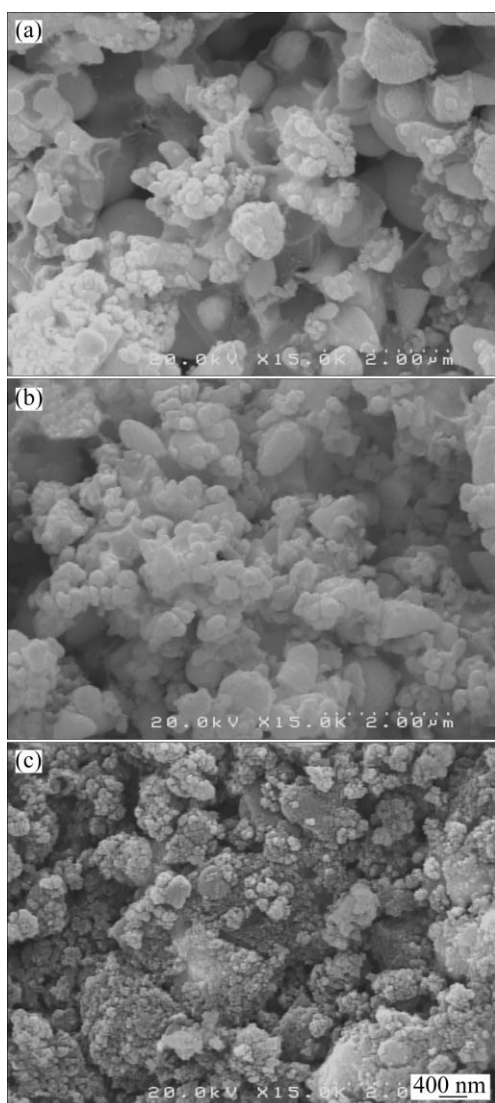


**Fig. 5** SEM images of products synthesized at microwave power of 600 W (a), 750 W (b) and 900 W (c)

and/or reagents) to captivate microwave energy and to change it into heat [36,37]. Two parameters represent the dielectric properties of a substance: the dielectric constant  $\epsilon''$ , explaining the ability to be polarized by the electric field, and the dielectric loss  $\epsilon'$ , describing the efficiency of electromagnetic radiation converted into heat [38]. The ratio of these two parameters describes the dielectric loss tangent,  $\tan \delta = \epsilon''/\epsilon'$ . This loss factor shows a measure for the ability of a material to convert electromagnetic energy into heat at a given frequency and temperature. A reaction medium with a high loss factor (high  $\tan \delta$  value) is suitable for efficient absorption and fast heating [39]. Polyalcohols like ethylene glycol, propylene glycol and glycerol [40], due to high loss tangents, are an appropriate solvents for microwave chemistry. Three different solvents were used to investigate the solvent effect on the morphology and particle size. As can be seen from Fig. 6(a), very regular

and small particles are obtained when ethylene glycol is used as solvent because of its high loss tangent (1.35) [41]. Ethylene glycol has the highest loss tangent and therefore it has the highest performance for irradiation to heating conversion. In fact, among three solvents, ethylene glycol solvent will provide sufficient energy and very fine particles will be obtained.

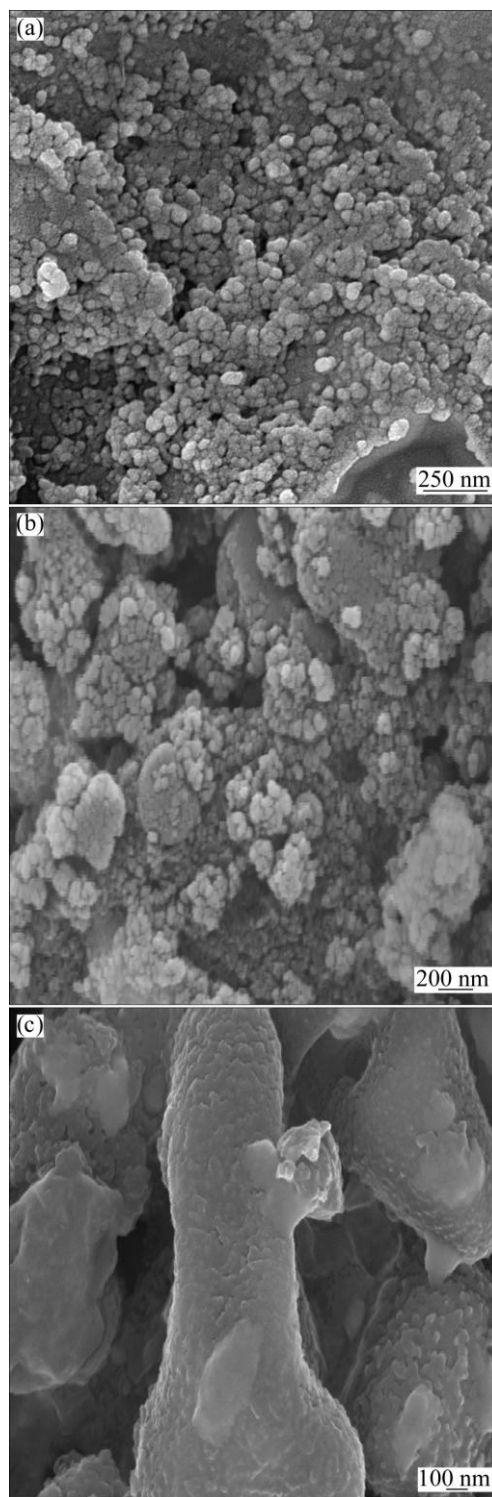


**Fig. 6** SEM images of products synthesized at 900 W for 5 min in different solvents: (a) Ethylene glycol; (b) Propylene glycol; (c) H<sub>2</sub>O

Propylene glycol as solvent has lower loss tangent (1.3) [42] in comparison with ethylene glycol, and the reaction medium has lower energy than the ethylene glycol medium. So, propylene glycol cannot provide required energy for precursors to prepare the product with small particles and hence larger and irregular particles are obtained (Fig. 6(b)).

In the long run, among the three solvents, the use of water with the lowest loss tangent (0.123) [42], due to providing the lowest energy, will lead to the formation of a bulk structure with micrometer size (Fig. 6(c)).

Figure 7 shows the relation between the size of particles and the concentrations of mercury ions and thio Schiff-base. It is observed that when the concentration of thio Schiff-base increases, the sizes of particles decrease and the optimum conditions are obtained at the molar ratio of  $\text{Hg}^{2+}$  to thio Schiff-base of 1:2. It is believed that when the reactants ratio increases, the nucleation rate increases, which leads to the formation of small nuclei at the same time (Fig. 7(a)). Further increase of this ratio may lead to agglomeration due to the formation of unstable and ultra-fine nuclei that have a strong tendency

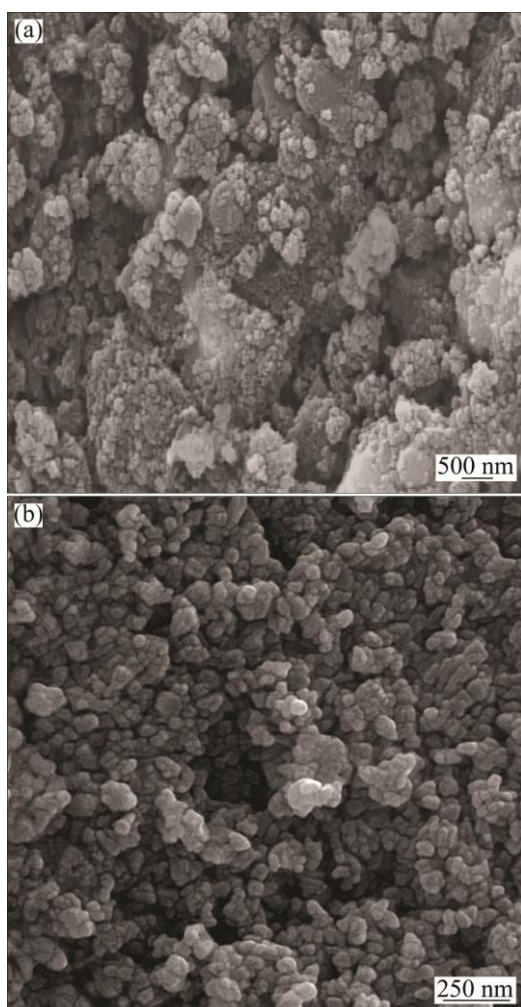


**Fig. 7** SEM images of products synthesized at 900 W for 5 min with different ratios of  $\text{Hg}^{2+}$  to sulfur source: (a) 1:2; (b) 1:4

to be stable by agglomeration. Therefore, the as-prepared HgS nanoparticles with molar ratio of  $\text{Hg}^{2+}$  to thio Schiff-base of 1:4 are large and dense (Fig. 7(b)). It should be noted that, product can not be formed in low content of thio Schiff-base (molar ratio of  $\text{Hg}^{2+}$  to thio Schiff-base of 1:1), because the nuclei are not sufficient for the formation of mercury sulfide at the same time.

UV–Vis absorption spectrum was carried out to investigate the optical properties of prepared HgS nanoparticles. Figure 8(a) shows the UV–Vis absorption spectrum of HgS nanoparticles synthesized via simple microwave approach at power of 900 W for 5 min in propylene glycol solvent. The sample has a strong absorbance in the ultraviolet region which is located at 356 nm.

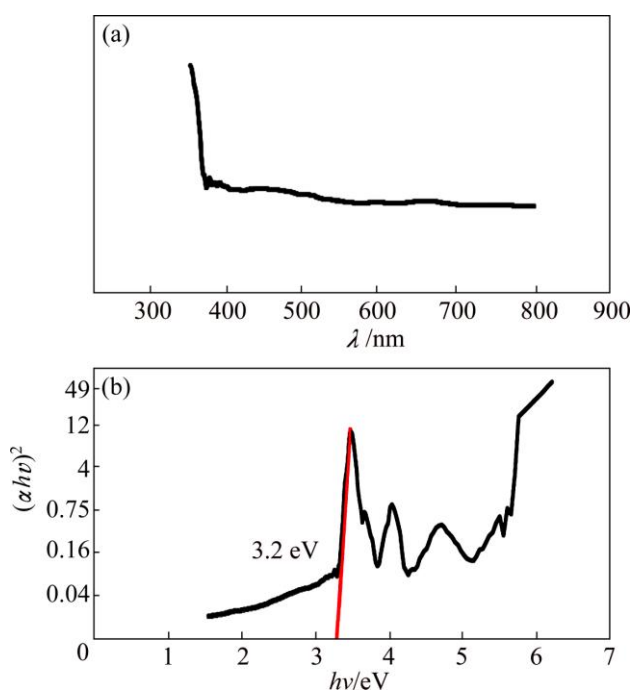


**Fig. 8** UV–Vis absorption spectrum of HgS prepared at 900 W for 5 min (a) and plot to determine direct band gap of HgS (b)

Figure 8(b) shows the plot of  $(\alpha hv)^2$  versus photon energy ( $hv$ ). For direct band gap materials, the absorption coefficient has the form of  $\alpha = A(hv - E_g)/hv$ , where  $A$  is a constant and  $E_g$  is the band gap. Thus, the optical band gap,  $E_g$ , can be calculated from the best linear approximation of  $(\alpha hv)^2$  versus  $(hv)$  plot, and its extrapolation to  $(\alpha hv)^2 = 0$ . HgS is a direct gap semiconductor with a band extremely located at the center of Brillouin zone [43]. As shown in Fig. 8(b), the band gap for HgS nanoparticles can be estimated to be 3.2 eV which has about 1.2 eV blue shift in comparison with the band gap of 2 eV for bulk sample [44]. Thus, the UV–Vis spectra have a blue shift probably due to smaller sizes of nanoparticles in comparison with that of bulk one [45–48].

## 4 Conclusions

1) The HgS nanostructures were synthesized by a microwave method from  $\text{Hg}(\text{OAc})_2$  and a new sulfuring agent from class of thio Schiff-base as starting material in the presence of propylene glycol as solvent. Systematic reaction conditions including kind of solvent, power of microwave oven, reaction time and precursor concentration on the size and morphology of obtained products were investigated.

2) The microwave method is proved to be simple and impressive. The use of toxic chemicals and time-consuming methods is avoided using the microwave method. This method brings forward a broad idea to synthesize other metal sulfides and sulfates with various morphologies and novel properties.

## Acknowledgments

The authors are grateful to council of University of Kashan for providing financial support to undertake this work by Grant No. 159271/368.

## References

- [1] KHANJANI S, MORSALI A. Synthesis and characterization of lanthanum oxide nanoparticles from thermolysis of nanostructured supramolecular compound [J]. *J Mol Liq*, 2010, 153(2–3): 129–132.
- [2] SADEGHZADEH H, MORSALI A. Synthesis of PbO nano-particles from a new one-dimensional lead(II) coordination polymer precursor [J]. *Mater Lett*, 2010, 64(7): 810–813.
- [3] YAZDANPARAST M S, MORSALI A. Sonochemical-assisted synthesis of nano-structured indium(III) hydroxide and oxide [J]. *Ultrason Sonochem*, 2011, 18(1): 375–381.
- [4] TOKYO N. Optical absorption and dispersion in rf-sputtered  $\alpha$ -HgS films [J]. *J Appl Phys*, 1975, 46(11): 4857–4861.
- [5] KALE S S, LOKHANDE C D. Preparation and characterization of HgS films by chemical deposition [J]. *Mater Chem Phys*, 1999, 59(3): 242–249.
- [6] DEBIAS G. Electrical and optical characterization of mixed layers of mercury sulphide [J]. *Phys Status Solidi A*, 1984, 83(1): 269–278.
- [7] COLVIN V L, SCHLAMP M C, ALVIASTORS A P. Light-emitting diodes made from cadmium selenide nanocrystals and a semiconducting polymer [J]. *Nature*, 1994, 370: 354–357.
- [8] HANGFELDT A, GRATZEL M. Light-induced redox reactions in nanocrystalline systems [J]. *Chem Rev*, 1995, 95(1): 49–68.
- [9] KALE S S, LOCKHANDE C D. Preparation and characterization of HgS films by chemical deposition [J]. *Mater Chem Phys*, 1999, 59(3): 242–246.
- [10] SHAO M, KONG L, LI Q, YU W, QIAN Y. Microwave-assisted synthesis of tube-like HgS nanoparticles in aqueous solution under ambient condition [J]. *J Inorg Chem Commun*, 2003, 6(6): 737–738.
- [11] XŪ Chang-qi, ZHANG Zhi-cheng, YE Qiang. A novel facile method to metal sulfide (metal=Cd, Ag, Hg) nano-crystallite [J]. *Mater Lett*, 2004, 58(11): 1671–1676.
- [12] ZHANG J, CHEN Z, WANG Z, MING N. The synthesis of HgS microcrystallites with controllable structure and morphology [J]. *Mater Res Bull*, 2004, 39(14–15): 2241–2247.
- [13] MUKHERJEE I, SENAPATI S, MITRA D, RAS A K, DAS S P, MOULIK S P. Physicochemistry of dispersions of HgO, HgS and ‘Makardhwaj’ (an Ayurvedic medicine) prepared in micelle and microemulsion templates [J]. *Colloids Surf A: Physicochem Eng Aspects*, 2010, 360(1–3): 142–149.
- [14] QIN D Z, MA X M, YANG L, ZHANG L. Biomimetic synthesis of HgS nanoparticles in the bovine serum albumin solution [J]. *J Nanopart Res*, 2008, 10(4): 559–564.
- [15] KRISTL M, DROFENIK M. Sonochemical synthesis of nanocrystalline mercury sulfide, selenide and telluride in aqueous solutions [J]. *Ultrason Sonochem*, 2008, 15(5): 695–699.
- [16] WANG H, ZHU J J. A sonochemical method for the selective synthesis of  $\alpha$ -HgS and  $\beta$ -HgS nanoparticles [J]. *Ultrason Sonochem*, 2004, 11(5): 293–300.
- [17] CHEN X, WANG X, WANG Z, YANG X, QIAN Y, CRYST J. Hierarchical growth and shape evolution of HgS dendrites [J]. *Growth*, 2005, 5(1): 347–353.
- [18] GUGLIELMI M, MARTUCCI A. Preparation and characterization of  $\text{Hg}_x\text{Cd}_{1-x}\text{S}$  and  $\text{Pb}_x\text{Cd}_{1-x}\text{S}$  quantum dots and doped thin films [J]. *J Sol-Gel Sci Technol*, 1998, 11: 229–235.
- [19] TOSHIKAZU O, YOSHIO S, SUSUMU N. Reaction temperature of HgS [J]. *Jpn J Appl Phys*, 1970, 9(3): 840–844.
- [20] MITCHELL M J, MUNIR Z A. Studies on the sublimation of IIB–VIA compounds. III. Equilibration and free surface pressures and enthalpies of sublimation of red mercury sulfide (cinnabar) [J]. *High Temp Sci*, 1970, 2(3): 265–273.
- [21] ZYLBERAJCH C. 2D monomolecular inorganic semi-conductors, inserted in a Langmuir–Blodgett matrix [J]. *Synth Met*, 1988, 27(3–4): 609–614.
- [22] ZYLBERAJCH C, RUAUDEL-TEIXIER A, BRRAUD A. Properties of inserted mercury sulphide single layers in a Langmuir–Blodgett matrix [J]. *Thin Solid Films*, 1989, 179(1–2): 9–14.
- [23] WANG H, ZHANG J R, ZHU J J. A microwave assisted heating method for the rapid synthesis of sphalerite-type mercury sulfide nanocrystals with different sizes [J]. *J Crystal Growth*, 2001, 233(4): 829–836.
- [24] LIAO X H, ZHU J J, CHEN H Y. Microwave synthesis of nanocrystalline metal sulfides in formaldehyde solution [J]. *Mater Sci Eng B*, 2001, 85(1): 85–89.
- [25] SASKIA A G. Microwave chemistry [J]. *Chem Soc Rev*, 1997, 26(2): 233–238.
- [26] GHADERI SHEIKHIABADI P, DAVAR F, SALAVATI-NIASARI M. The single source preparation of rod-like mercury sulfide nanostructures via hydrothermal method [J]. *Inorganica Chimica Acta*, 2011, 376(1): 271–280.
- [27] LI Y D, DING Y, LIAO H W, QIAN Y T. Room-temperature conversion route to nanocrystalline mercury chalcogenides  $\text{HgE}$  ( $\text{E}=\text{S}, \text{Se}, \text{Te}$ ) [J]. *J Phys Chem Solids*, 1999, 60(7): 965–968.
- [28] ZHANG H, YANG D, LI S, JI Y, MA X, QUE D. Hydrothermal synthesis of flower-like  $\text{Bi}_2\text{S}_3$  with nanorods in the diameter region of 30 nm [J]. *Nanotechnology*, 2004, 15(9): 1122–1125.
- [29] JENKINS R, SNIDER R L. Chemical analysis: Introduction to X-ray powder diffractometry [M]. New York: John Wiley & Sons, Inc, 1996.
- [30] SALAVATI-NIASARI M, BAZARGANIPOUR M, DAVAR F. Simple sonochemical synthesis and characterization of HgSe nanoparticles [J]. *Ultrason Sonochem*, 2012, 19(5): 1079–1086.
- [31] MEDIIVILLA M, MORALES H, MELO L, SIFONTES A B, ALBORNOZ A, LLANOS A, MORONTA D, SOLANO R, BRITO J L. Microwave-assisted polyol synthesis of Pt/H-ZSM5 catalysts [J]. *Microporous and Mesoporous Materials*, 2010, 131(1–3): 342–349.
- [32] XIONG Y J, XIE Y, DU G A, SU H L. From 2D Framework to Quasi-1D nanomaterial: Preparation, characterization, and formation mechanism of  $\text{Cu}_3\text{SnS}_4$  nanorods [J]. *Inorg Chem*, 2002, 41(11): 2953–2959.

- [33] SHELDRIK W S, WACHHOLD M. Solventothermal synthesis of solid-state chalcogenidometalates [J]. *Angewandte Chemie International Edition*, 1997, 36(3): 206–224.
- [34] VRANKA R G, AMMA E L. Electron-deficient bonding involving sulfur atoms. II. The crystal structure of  $\text{Cu}_4[\text{SC}(\text{NH}_2)_2]_9(\text{NO}_3)_4$  [J]. *J Am Chem Soc*, 1966, 88(18): 4270–4271.
- [35] LU J, HAN Q, YANG X, LU L, WANG X. Microwave-assisted synthesis and characterization of 3D flower-like  $\text{Bi}_2\text{S}_3$  superstructures [J]. *Mater Lett*, 2007, 61: 2883–2886.
- [36] KAPPE C O. Controlled microwave heating in modern organic synthesis [J]. *Angewandte Chemie International Edition*, 2004, 43(46): 6250–6284.
- [37] KAPPE C O, DALLINGER D, MURPHREE S S. Practical microwave synthesis for organic chemists [M]. Weinheim: Wiley-VCH, 2009.
- [38] MICHAEL D, MINGOS P, BAGHURST D R. Tilden lecture. Applications of microwave dielectric heating effects to synthetic problems in chemistry [J]. *Chem Soc Rev*, 1991, 20(1): 1–47.
- [39] BILECKA I, NIEDERBERGER M. Microwave chemistry for inorganic nanomaterials synthesis [J]. *Nanoscale*, 2010, 2(8): 1358–1374.
- [40] GABRIEL C, GABRIEL S, GRANT E H, HALSTEAD B S J, MINGOS D M P. Dielectric parameters relevant to microwave dielectric heating [J]. *Chem Soc Rev*, 1998, 27(3): 213–224.
- [41] HAYES B L. Microwave synthesis: Chemistry at the speed of light [M]. Matthews NC: CEM Publishing, 2002.
- [42] TIERNEY J P, LIDSTROM P. Microwave assisted organic synthesis [M]. New Delhi: Wiley, 2009.
- [43] HENDERSON D O, MU R, UEDA A, WU M H, GORDON E M, TUNG Y S, HUANG M, KEAY J, FELDMAN L C, HOLLINGSWORTH J A, BUHRO W E, HARRIS J D, HEPP A F, RAFFAELLE R P. Optical and structural characterization of copper indium disulfide thin films [J]. *Materials and Design*, 2001, 22(7): 585–589.
- [44] TAUC J, MENTH A. States in the gap [J]. *Non Cryst Solids*, 1972, 8: 569–585.
- [45] GHANBARI D, SALAVATI-NIASARI M, KARIMZADEH S, GHOLAMREZAEI S. Hydrothermal synthesis of  $\text{Bi}_2\text{S}_3$  nanostructures and ABS-based polymeric nanocomposite [J]. *Journal of Nano Structures*, 2014, 4(2): 227–232.
- [46] NABIYOUNI G, SHARIFI S, GHANBARI D, SALAVATI-NIASARI M. A simple precipitation method for synthesis  $\text{CoFe}_2\text{O}_4$  nanoparticles [J]. *Journal of Nano Structures*, 2014, 4(3): 317–323.
- [47] PANABI-KALAMUEI M, MOUSAVI-KAMAZANI M, SALAVATI-NIASARI M. Facile hydrothermal synthesis of tellurium nanostructures for solar cells [J]. *Journal of Nano Structures*, 2014, 4(4): 459–465.
- [48] BESHKAR F, SALAVATI-NIASARI M. Facile synthesis of nickel chromite nanostructures by hydrothermal route for photocatalytic degradation of acid black 1 under visible light [J]. *Journal of Nano Structures*, 2015, 4(1): 17–23.
- [49] NEJATI-MOGHADAM L, ESMAEILI BAFGHI-KARIMABAD A, SALAVATI-NIASARI M, SAFARDOUST H. Synthesis and characterization of  $\text{SnO}_2$  nanostructures prepared by a facile precipitation method [J]. *Journal of Nano Structures*, 2015, 5(1): 47–53.

## 通过简单微波法使用新型硫化剂制备 HgS 纳米颗粒的结构与光谱表征

Hossein SAFARDOUST-HOJAGHAN<sup>1</sup>, Maryam SHAKOURI-ARANI<sup>2</sup>, Masoud SALAVATI-NIASARI<sup>1</sup>

1. Institute of Nano Science and Nano Technology, University of Kashan, Kashan, P.O. Box 87317-51167, Iran;

2. Department of Chemistry, Payame Noor University, Tehran, P.O. Box 19395-3697, Iran

**摘要:** 通过简单的微波反应, 使用一种新型的前驱体复合物 $[\text{Hg}(\text{C}_{13}\text{H}_{11}\text{NSO})_2]^{2+}$ , 制备具有不同形貌和颗粒尺寸的晶体汞硫化物(HgS)。通过 X 射线、扫描电镜、紫外-可见光谱对产物进行表征, 获得了具有不同尺寸的汞硫化物纳米结构。研究前驱体浓度、溶剂种类、微波时间和功率对产物尺寸和形貌的影响。结果表明: 溶剂种类和微波功率极大地影响 HgS 的最终尺寸。乙二醇是合成细小颗粒 HgS 的最佳溶剂, 制备具有尺寸分布均匀的 HgS 纳米颗粒的最佳功率是 900 W。通过紫外-可见光谱计算出 HgS 纳米颗粒的带隙是 3.2 eV, 这相对于块体样品 2 eV 的带隙蓝移了 1.2 eV。

**关键词:** 汞硫化物; 微波法; 纳米结构; 含硫席夫碱

(Edited by Mu-lan QIN)